

## Valence Space Techniques and QRPA Vibrational Mass Parameters

**I. Deloncle<sup>1,2</sup>, F. Lechaftois<sup>1</sup>, S. Péru<sup>1</sup>**

<sup>1</sup>CEA, DAM, DIF 91680 Arpajon, FRANCE

<sup>2</sup>CSNSM, IN2P3/CNRS, 91405 Orsay Campus, FRANCE

**Abstract.** The vibrational mass parameters entering the quadrupolar 5DCH Hamiltonian are commonly calculated neglecting beyond mean-field correlations and dynamical rearrangement of the self-consistent field [1]. The Quasiparticle Random Phase Approximation (QRPA) framework would allow to avoid the aforementioned approximations. However, due to prohibitive computation time, in particular when using finite-range interactions such as Gogny ones, the calculation of QRPA mass parameter is unrealisable. In order to reduce the QRPA computation time valence space techniques are applied, leading to a gain in time of a factor up to 30. The convergence properties of the calculated mass parameters prove their robustness toward the valence space limitations. On the contrary, the intrinsic QRPA outputs exhibit weak convergence properties, with deceptive appearance when inserting an inert core. Therefore, for the optimization of the valence space limits neither the excited states energy, nor the associated transition probabilities, should be considered for criteria of convergence.

### 1 Introduction

In the 5DCH theory the Bohr Hamiltonian is built and solved microscopically, without any free parameter. Starting from only one ingredient – a density-dependent force (the D1M Gogny interaction in the present work)– the low-energy quadrupolar dynamics, involving five collective degrees of freedom, is obtained from self-consistent mean-field solutions. The reduction of the computation time, relatively to the GCM process, obtained thanks to the GOA approximation makes 5DCH a possible cornerstone for the construction of an “universal” approach describing, on the same foot and from only one nucleon-nucleon interaction, nuclei along the whole chart. Indeed, as soon as the concept of mean-field is meaningful (for  $N, Z \gtrsim 10$ ), 5DCH calculations can be undertaken in light nuclei, as well as in the heaviest ones for which the computation time is manageable. It is worth recalling that this approach is not limited to axial symmetry, and implies a  $\beta, \gamma$  mapping. Yet, several drawbacks of 5DCH are known [1, 2], giving rise to a dependence of the result reliability on the nuclear deformation. Possible cure of 5DCH could be obtained by adding beyond mean-field correlations to the 5DCH vibrational mass parameters [1–4]. In principle that could be achieved in Quasiparticle Random Phase Approximation (QRPA),

but not in practice due to the prohibitive QRPA time consumption, in particular when using a density-dependent force. On another hand, the strong variations with the deformation of the vibrational mass parameters [5, 6] impose to compute them for a large amount of  $\beta, \gamma$  values. The time related cost is then a key issue in the development of 5DCH cures, and our recent work, in that respect, represents an important breakthrough. Indeed, for the first time a vibrational mass parameter is obtained, in a reasonable computational time, within a HFB+QRPA approach built on a Gogny interaction. In this work, the computing time reduction is obtained by setting limitations on the valence space available for the excitations entering the QRPA calculations. The technique of the cut-off in the 2 quasi-particle (qp) energy, that imposes a limit in the upper single level involved in 2qp excitation, has already been validated for phonon energy, with Skyrme [7] as well as with D1S [8]. Here we explore its consequence on mass parameter.

Another way of limiting the valence space is used in standard shell model: the introduction of an inert core that put aside the lowest single-particle levels. We apply this technique for the first time in QRPA calculations.

Both the 2qp energy cut-off and the inert core size are determined according to the convergence of the mass parameter calculations. It is compared to the one observed for the built-in QRPA outputs, namely phonon energies and reduced transition probabilities.

## 2 Formalism for Vibrational Mass Parameters

### 2.1 Form TDHFB to Inglis-Belyaev

In 5DCH calculations, the potential energy  $V$ , the three moments of inertia  $\mathfrak{J}_i$  (with  $i \in (x, y, z)$ ) and the three vibrational mass parameters  $B_{\mu\nu}$  (with  $(\mu, \nu) \in (0, 2)$ ) of the Bohr Hamiltonian

$$\mathcal{H} = V + T_{rot} + T_{vib} \quad (1)$$

$$T_{rot} = \frac{1}{2} \sum_i \mathfrak{J}_i \omega_i^2 \quad (2)$$

$$T_{vib} = \frac{1}{2} (B_{00} \dot{q}_0^2 + B_{22} \dot{q}_2^2 + B_{02} \dot{q}_0 \dot{q}_2) \quad (3)$$

are determined microscopically at few tens of points of the sextant ( $\beta, 0^\circ \leq \gamma \leq 60^\circ$ ) from constrained Hartree-Fock-Bogolyubov (CHFB) calculations.

Usually the vibrational mass parameters are computed at the cranking order using the Inglis-Belyaev formula. This formula is established from time dependent Hartree-Fock (TDHFB) framework when making two assumptions. First, the adiabaticity of the collective motion (ATDHFB). It allows a perturbative development of the generalised density, that one stops at the first order (cranking order). Moreover one neglects the modification of the mean-field brought by the perturbation of the density. Indeed, the first order term modifying the mean-field is time-odd. Its inclusion would impose to break the time reversal symmetry,

essential for the pairing treatment. As a result, the Inglis-Belyaev formula requires only static ingredients, obtained in CHFb calculations. The dynamics is “restored” only by the 5DCH diagonalisation. Indeed, in the Gaussian Overlap Approximation (GOA), as in the Generalized coordinate method, the eigenstates of the Bohr Hamiltonian are sought as superposition of CHFb states. By mixing CHFb states from different deformation, one mixes different single-particle level configuration (or quasiparticle occupation  $u, v$ ). An empty orbital on the prolate side may be below the Fermi level at oblate deformation. Many configurations, that excitations would involve, are thus explored with deformation. These are the configurations, or HFB states, with similar “mechanical” energy of the 5DCH Hamiltonian (sum of  $V$  and  $T_{vib}$ ) that will be mixed in a vibrational state solution of 5DCH. Now, a vibrational mass parameter, sensitive to the underlying single-particle structure, often presents large variations with deformation, some peaks with huge value. At the deformation where peaks appear, the  $\hbar^2/2B$  term of the requantized 5DCH Hamiltonian will then be very small allowing to compensate the high potential energy of configurations at this deformation. They will take part in the low-energy dynamics. This is the way that mass parameters drive the deformation of the 5DCH eigenstates, and low-energy excited states can be deformed despite a spherical HFB minimum as in Tin isotopes [4, 9] or in  $^{32}\text{Mg}$  [10] for example. The mass parameters are then crucial physical quantities for the whole dynamics, and it is essential to improve their modelling, to include the dynamical mean-field rearrangement, to enrich their content with correlations beyond the mean-field as well. Indeed, the mean-field is a static and a particle independent (as uncorrelated) view of the nucleus. Only a part of the correlations brought by the interaction can be included (averaged) in the mean-field construction, many are neglected. The pairing for example, that affects the mass parameters, is included after each iteration in BCS calculations, or requires the quasiparticle formalism to be included in mean-field calculations. The Quasiparticle Random Phase Approximation (QRPA), since taking into account 2 qp correlations that do not enter the HFB formalism (residual interaction), is a possible path toward enriched vibrational mass parameter.

## 2.2 From TDHFB to QRPA

QRPA is another limit of the TDHFB, the small amplitude limit. It provides a formalism to study the harmonic answer of a nucleus when submitted, at the equilibrium (at the minimum of potential energy), to a small impulsion. This answer is sought as coherent (or correlated) superpositions of 2qp excitations, the phonons. The phonon creation operator is given by:

$$\theta_n^+ = \sum_{kk'} (X_{kk'}^n \alpha_k^+ \alpha_{k'}^+ - Y_{kk'}^n \alpha_k \alpha_{k'}), \quad (4)$$

$$\theta_n^+ |\text{QRPA}\rangle = |n\rangle \quad (5)$$

In the creation of a phonon, 2qp are deleted and (re)created together with different X and Y amplitudes. The amplitudes are solutions of the equation:

$$\begin{pmatrix} A & B \\ B^* & A^* \end{pmatrix} \begin{pmatrix} X_n \\ Y_n \end{pmatrix} = \omega_n \begin{pmatrix} X_n \\ -Y_n \end{pmatrix} \quad (6)$$

the matrix elements of A and B are calculated from the residual interaction.

Nearly forty years ago, Vautherin [11] established the equivalence of the ATHFB mass parameter (built from a mean-field with a constraint on an operator related to the nuclear polarizability) and the cubic inverse energy weighted RPA sum rule :

$$B_{\mu\nu} = \frac{\hbar^2}{2} \frac{\mathcal{M}_{-3}(Q_{\mu\nu})}{\mathcal{M}_{-1}(Q_{\mu\nu})}, \quad (7)$$

with  $\mu, \nu \in (0, 2)$ , for  $q_0$  and  $q_2$ .

The  $k^{th}$  order moment of the  $Q_{\mu\nu}$  strength distribution is given by:

$$\mathcal{M}_k(Q_{\mu\nu}) = \sum_n \omega_n^k |\langle \phi | \theta_n^+ Q_{2\mu} | \phi \rangle \langle \phi | \theta_n^+ Q_{2\nu} | \phi \rangle| \quad (8)$$

Unfortunately, as already mentioned the calculation time prevents the use of QRPA, as it is, for the 5DCH mass parameter. In the following, we restrict the number of 2qp excitations entering in Eq. (5) in order to evaluate Eq. (7).

### 3 Results

The study is performed on the  $^{110-144}\text{Sn}$  isotopes, exploring with the neutron number a variety of underlying single-particle level spectrum as large as the one encountered in one nucleus as a function of deformation. The  $^{110-144}\text{Sn}$  isotopes have a minimum of HFB energy at zero deformation, where the QRPA and the mass parameter calculations will be performed. It allows to decorrelate the notion of valence space from deformation. Moreover, at zero deformation the  $B_{\mu\nu}$  fulfil the relation:

$$B_{00} = \frac{\hbar^2}{2} \frac{\mathcal{M}_{-3,00}}{[\mathcal{M}_{-1,00}]^2} = 2B_{20} = 4B_{22}. \quad (9)$$

Our study can then be realized on  $B_{00}$  only. The quasi particles, inputs of the QRPA process, have been determined with the axial HFB code of ref. [12]. In HFB as well as in QRPA calculations, the effective interaction is DIM [13] and an harmonic oscillator basis with 11 major shells is used, checked to be sufficient for convergence in the  $^{100-144}\text{Sn}$  isotopes. The axial QRPA calculation have been achieved with the multi threads version [8] of the code introduced in [14]. The restriction of the qp entering the QRPA calculation is done by defining, in the whole matrix, QRPA sub-matrix, for which the diagonalization, that is the fastest part of the QRPA process, is performed.

### 3.1 Mass parameter with 2qp energy cut-off

In this section, the reduction of the valence space is realized by setting an energy cut-off on the 2qp excitations (i.e the sum of the energies of the qp involved in the excitation). Are considered only 2qp excitations with energy below or equal that of the cut-off. If the assumption that high energy 2qp excitation do not play a major role in the nuclear polarizability is correct, it should exist a cut-off value providing a reasonable approximation of the value obtained without any valence space restriction,  $B_{00\emptyset}^{\text{no core}}$ , our absolute reference (full QRPA). (The symbol  $\emptyset$  is used in this paper to indicate calculations without any cut-off)

In Figure 1 is drawn  $R(B_{00})=B_{00,\text{cut}}^{\text{no core}}/B_{00\emptyset}^{\text{no core}}$  as a function of  $A$ . The choice of a 2qp energy cut-off above 50 MeV is immediate. Below 50 MeV the  $B_{00,\text{cut}}^{\text{no core}}$  values lie between 1.5 up to 13.5 times the  $B_{00\emptyset}^{\text{no core}}$  one. On the contrary, convergence is obtained with energy cut-offs from 50 MeV. In the insert of the Figure 1, more than 90% in mean (with one exception,  $^{130}\text{Sn}$ ) of the reference value is reached with 50-MeV cut-off. It would be interesting to get more information in the intermediate 20-50 MeV energy range, by setting for example a 40 MeV cut-off. This is in progress.

One can also note in Figure 1 effects due to the underlying single-particle level density. For small energy cut-off, the curves present typical shell effects, large peaks at shell closures. Between  $A=100$  and  $A=132$ , 2qp benefit by the shells lying between the gaps, to generate excitations with little energy. This leads to the parabolic shape of the curves, with a minimum around  $N=62$  ( $\nu g_{7/2}$  occupancy). The curves corresponding to 10, 15 and 20 MeV cut-offs are superimposed, thus 2qp excitations with at most 10 MeV are dominating. Their little energy makes them ineffective at shell closure. At the contrary, the 2qp excitation with 15-20 MeV energy survive the proximity of the  $N=82$  gap. One can note also better values obtained in  $^{126-144}\text{Sn}$  with a 20 MeV cut-off, in particular the stiff drop of the corresponding curve (in magenta) from above 5, for

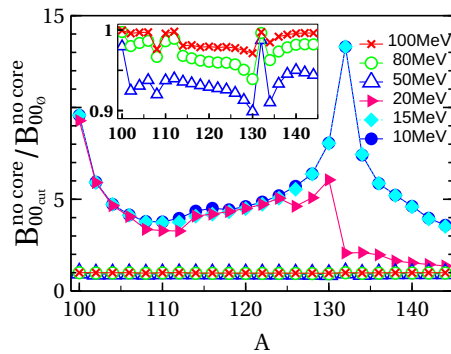


Figure 1. For different 2qp energy cut-off values and as a function of mass, ratio  $R(B_{00})$  (see text). A zoom on the ordinate around the value of 1.0 is shown in the insert.

$A=130$ , to below 2 for heavier mass  $A \geq 132$ . In  $^{132-144}\text{Sn}$  (from  $N \geq 82$ ), the inclusion of the 15-20 MeV range of 2qp excitations reduces significantly the overestimation of the mass parameter observed with lower energy cut-offs. In these isotopes, these only excitations, with rather low energy, give mass parameter lying below twice the reference. These excitations are not hindered at the  $N=82$  shell gap, when they are at  $N=50$ . All these features indicate that 2qp excitations with “low” energy carry fine nuclear structure information, they can not be neglected. Therefore, the use of a high- and low-cut filter for computing vibrational mass parameter is excluded.

It is worth noting that in Tamm-Dancoff approximation, one obtains  $B_{00\text{TDA}}$  greater than  $B_{00\emptyset}^{\text{no core}}$  in all Sn isotopes [16]. The ratio (1.3 in mean) presents also variations as a function of  $A$ , with a minimum at  $N=82$  shell closure (near 1.1). Neglecting 2qp excitations with energy higher than 20 MeV, or ground-state correlations, results in an overestimated mass parameter  $B_{00}$ .

Inversely, from 50-MeV cut-off the obtained mass parameters are satisfactory underestimate of the expected value. With one exception, the results of the insert of Figure 1 lie above 90% of the reference value. Discrepancies are obtained at the beginning of the  $\nu g_{7/2}$  occupancy, and near shell closure whereas at the shell closures, 99% of the reference value is reached with cut-off from 50 MeV. In our previous work  $B_{00\text{Inglis-Belyaev}}$  commonly used in 5DCH, was found, 1.3 times in mean smaller than  $B_{00\emptyset}^{\text{no core}}$ , with a larger discrepancy at shell closure.

The valuable results obtained with a 50-MeV energy cut-off validates our hypothesis : the high energy 2qp excitations play a minor role only in the mass parameter value. Moreover, a 50-MeV energy cut-off provides a reduction in computation time of a factor 16. In the following we detail an approximation to be used with the 2qp energy cut-off technique and that will allow us to gain an additional factor in computation time.

### 3.2 Mass parameter with inert core

Never applied in QRPA, but largely and commonly used in standard shell model calculation, is the technique consisting in freezing the deep qp lying at the bottom of the mean-field, in an inert (non excitable) core. We directly imported this technique in our QRPA calculations and build submatrices by selecting qp that are rows and columns of the whole QRPA matrices.

We performed the calculations with five different cores,  $^{40}\text{Ca}$ ,  $^{48}\text{Ca}$ ,  $^{56}\text{Ni}$ ,  $^{70}\text{Ca}$ , and  $^{78}\text{Ni}$ . The results obtained with the two first cores are sufficient to draw conclusions. On Figure 2 are only reported the ratios  $R_{abs}(B_{00})$  of  $B_{00\text{cut}}^{40\text{or}48\text{Ca}}$  over  $B_{00\emptyset}^{\text{no core}}$  obtained with the whole QRPA matrix.

A common feature appears at a first glance in the results drawn in Figure 2: the dramatic change in the slope and values of the curves when the energy cut-off reaches 50 MeV. Below, the mass parameter are overestimated, the slopes exhibit important variations according to the neutron number. Above, only slight variations are observed (see inserts). However, in the inserts on the left panel the

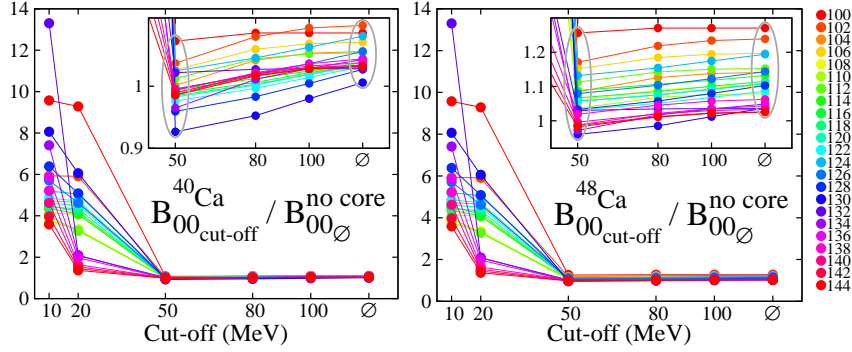


Figure 2. As a function of the cut-off value, ratios  $R_{\text{abs}}(B_{00})$  (see text) in  $^{100-140}\text{Sn}$  isotopes for two different inert cores. The color to mass correspondence is given by the palette at the right. A zoom on ordinate is shown in the insert. Ellipses allow to highlight the convergence of the curves toward themselves.

curves merge toward each other when converging to relevant no cut-off values – lying within 90 percent of the  $B_{00}^{\text{no core}}$ , our reference–. In the right panel the “inter convergence” of the curves toward each other is less pronounced, as is less pronounced their own convergence to their less acceptable asymptotic values, ranging between 1.05 and 1.25. With the heavier inert cores, the curves diverge between themselves. Such effect may be of great interest to check the pertinence of the convergence process.

In Table 1, are reported the mean value and the standard deviation of the asymptotic values of the ratio  $R_{\text{abs}}(B_{00}) = B_{00}^{\text{core}} / B_{00}^{\text{no core}}$  obtained for different cores without energy cut-off.

All the asymptotic values are, from  $^{56}\text{Ni}$ , large overestimations (by a factor at least 1.15) of the mass parameter. In this paper, overestimation was previously observed when neglecting ground-state correlation or 2qp excitation with energy below, or equal to, 50 MeV. This of course is due to the inert core insertion, which reduces *de facto* ground-state correlations, since many qp are not participating anymore to Eqs (6) and (8). Frozen in large inert core ( $N, Z \geq 28$ ), there are not so deep qp that would have participated to in-shells excitations with intermediate energy. Their excitation toward shell above the Fermi level would require very high energy.

Table 1. Mean value and standard deviation of the distribution over the  $^{100-144}\text{Sn}$  isotopes of the asymptotic values of  $R_{\text{abs}}(B_{00})$  according to the different inert cores

	$^{40}\text{Ca}$	$^{48}\text{Ca}$	$^{56}\text{Ni}$	$^{70}\text{Ca}$	$^{78}\text{Ni}$
mean val.	1.04	1.11	1.24	1.53	1.70
stdev	0.02	0.07	0.09	0.29	0.34

With a  $^{48}\text{Ca}$  inert core, few Sn isotopes have a mass parameter slightly underestimated when using a 50-MeV energy cut-off, see Figure 2. They also have asymptotic values lying very near the reference. For these isotopes it should be possible to take benefit of the  $^{48}\text{Ca}$  inert core to reduce more drastically the computation time.

Of course, for systematic calculations, the results summed up in Table 1 and Figure 2 rule out the use of any core heavier than  $^{40}\text{Ca}$  in combination with a 50-MeV cut-off. Fortunately, the computation time is significantly reduced, by a factor 2, when using this inert core. When applying, in addition, a 50-MeV energy cut-off the total gain in computation time reaches a factor 30. If these two approximations are robust, it should give room enough for facing calculations of QRPA mass parameters, with a valence space, in most of the nuclei at any deformation. In order to check the robustness of our mass parameter, and to assess our hypothesis, calculations of intrinsic QRPA outputs, i.e. phonon energy and their reduced transition probability with valence space have been undertaken.

### 3.3 QRPA outputs with 2qp energy cut-off

In Figure 3 are drawn as a function of the 2qp energy cut-off, the variation of the  $2_1^+$  and  $3_1^-$  energies, and of their associated reduced transition probability, relatively to the reference values obtained without cut-off (and no core). Opposite trends are observed for the excited state energies and the transition probabilities.

At 50 MeV, neither the energies nor the transition probabilities are converged. The convergence is only obtained from 80 MeV (100 MeV) cut-off for the  $2_1^+$  ( $3_1^-$  respectively) energy and transition probability. The 2qp excitations with energy lower or equal to 50 MeV that make 90% of the vibrational

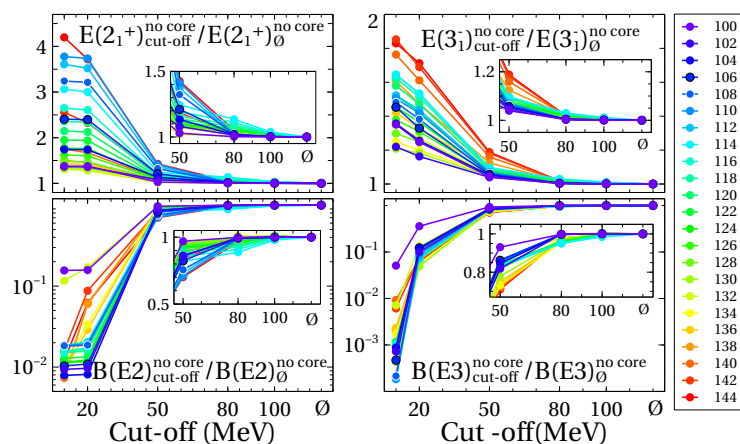


Figure 3. As a function of the cut-off value, ratios determined with cut-off over reference value, in  $^{100-140}\text{Sn}$  isotopes. The color to mass correspondence is given in the palette at the right. A zoom on the ordinate around the value of 1.0 is shown in the insert.

mass parameter  $B_{00}$  represent of the order of 70% only of what is needed to build the first excited states. The lack of high-energy 2qp excitations has heavy consequences. Inversely, it confirms their secondary role in the polarizability.

In Figure 3, one can also notice, on the one hand, the greater sensitivity of the transition probability, as compared to the excited state energy, to missing 2qp excitations with energy comprised between 20 and 50 MeV, and on the other hand, the necessity to include 2qp excitation of even lower energy, between 10 and 20 MeV, for an accurate calculation of the  $B(E3)$ .

### 3.4 QRPA outputs with inert core

In Table 2, are reported the mean value and the standard deviation of the asymptotic values (i.e without energy cut-off) of the ratios  $R_{\text{abs}}(X)=X_{\emptyset}^{\text{core}}/X_{\emptyset}^{\text{no core}}$ , where  $X$  stands for  $E(2_1^+)$  or  $E(3_1^-)$ , obtained with different cores. Once more the results for the  $2_1^+$  differ from those for the  $3_1^-$ . The latter that exhibit better convergence properties though not sufficient to give valuable results with any of the cores used here. It is worth noting that we obtained satisfactory values for both state energies when using a much smaller inert core,  $^{16}\text{O}$ .

Table 2. Mean value and standard deviation of the distribution over the  $^{100-144}\text{Sn}$  isotopes of the asymptotic values of  $R_{\text{abs}}(E(2_1^+))$  and  $R_{\text{abs}}(E(3_1^-))$  obtained with different inert cores

		$^{40}\text{Ca}$	$^{48}\text{Ca}$	$^{56}\text{Ni}$	$^{70}\text{Ca}$	$^{78}\text{Ni}$
$E(2_1^+)$	mean val.	1.39	1.47	1.65	1.70	1.79
	stdev	0.31	0.36	0.49	0.54	0.61
$E(3_1^-)$	mean val.	1.16	1.19	1.27	1.30	1.34
	stdev	0.06	0.07	0.10	0.11	0.13

As a last result is shown in Figure 4 the remarkable deceptive convergence scheme of the relative ratio  $R_{\text{rel}}(E(2_1^+))$  of  $E(2_1^+)_{\text{cut-off}}^{\text{core}}$  over  $E(2_1^+)_{\emptyset}^{\text{core}}$  obtained with  $^{78}\text{Ni}$  as inert core. The convergence toward the asymptotic no cut-off value obtained with a given core has the appearance of a fast and efficient process, despite large difference between the asymptotic no cut-off value obtained with a core at a given mass and the absolute value with no cut-off, no core.

These results are astonishing since in standard shell models calculations larger cores are commonly used. It would be possible to perform the required normalizations (on each multipolarity) since we can get the absolute value – full QRPA calculations are always possible –. That would be, however, counter productive since time-consuming and would lead to the loss of the “universal” and coherent character of the 5DCH approach, which, starting from one density-dependent force only, aims to describe nuclei over the whole chart.

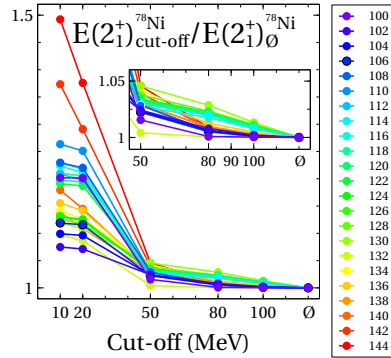


Figure 4. As a function of the cut-off value, ratios  $R_{\text{rel}}(E(2_1^+))$  (see text) in  $^{100-140}\text{Sn}$  isotopes for the  $^{78}\text{Ni}$  inert core. The color to mass correspondence is given by the palette at the right. A zoom on ordinate is provided in the insert.

## 4 Conclusions

The introduction of the valence space notion in QRPA calculations, via  $2\text{qp}$  energy cut-off and inert core, is an important breakthrough for the 5DCH framework. It offers a glimpse of a possible path toward valuable vibrational mass parameter calculations on few tens of  $(\beta, \gamma)$  points. The vibrational mass parameters appear very robust against valence space limitations, allowing a factor of 30 to be reached in the computation time reduction. On the contrary, unreliable values are obtained for intrinsic QRPA outputs in the same approximations, that exhibit deceptive convergence.

## References

- [1] J.-P. Delaroche, M. Girod, J. Libert, H. Goutte, S. Hilaire, S. Péru, N. Pillet and G.F. Bertsch, *Phys. Rev. C* **81** (2010) 014303.
- [2] G.F. Bertsch, M. Girod, S. Hilaire, J.-P. Delaroche, H. Goutte and S. Péru, *Phys. Rev. Lett.* **99** (2007) 032502.
- [3] M. Bender and P.-H. Heenen, *Phys. Rev. C* **78** (2008) 024309.
- [4] S. Péru and M. Martini, *Eur. Phys. J. A* **50** (2014) 88.
- [5] B. Mohammed-Azizi, *Electronic J. Theor. Phys.* **9** (2012) 143-158.
- [6] E.Kh. Yuldashbaeva, J. Libert, P. Quentin and M. Girod, *Phys. Lett. B* **461** (1999) 1.
- [7] K. Yoshida and N. Van Giai, *Phys. Rev. C* **78** (2008) 064316.
- [8] S. Péru, G. Gosselin, M. Martini, M. Dupuis, S. Hilaire and J.-C. Devaux, *Phys. Rev. C* **83** (2011) 014314.
- [9] J. Libert, B. Roussière and J. Sauvage, *Nucl. Phys. A* **786** (2007) 47.
- [10] S. Péru, M. Girod and J.-F. Berger, *Eur. Phys. J. A* **9** (2000) 35.

*Valence Space Techniques and QRPA Vibrational Mass Parameters*

- [11] D. Vautherin, *Phys. Lett.* **69B** (1977) 393.
- [12] S. Hilaire and M. Girod, *Eur. Phys. J. A* **33** (2007) 237.
- [13] S. Goriely, S. Hilaire, M. Girod and S. Péru, *Phys. Rev. Lett.* **102** (2009) 242501.
- [14] S. Péru and H. Goutte, *Phys. Rev. C* **77** (2008) 044313.
- [15] J. Libert, M. Girod and J.-P. Delaroche, *Phys. Rev. C* **60** (1999) 054301.
- [16] F. Lechaftois, I. Deloncle and S. Péru, *Phys. Rev. C* **92** (2015) 034315.